iScience

CellPress
OPEN ACCESS

Article

Cervical transcutaneous spinal stimulation for spinal motor mapping

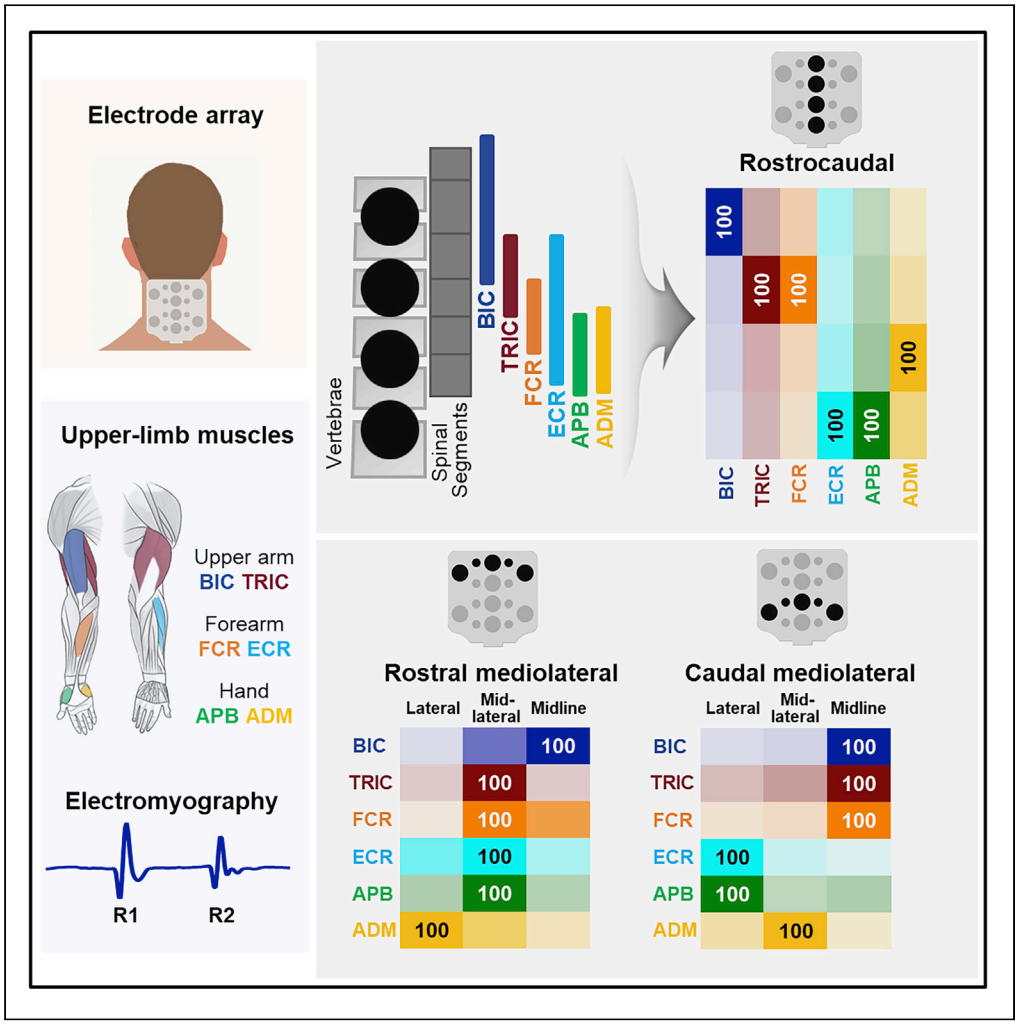

Jeonghoon Oh, Alexander G. Steele, Blesson Varghese, ..., Rachel L. Markley, Yi-Kai Lo, Dimitry G. Sayenko

dgsayenko@houstonmethodist.org

Highlights

Cervical spinal motor maps are created by transcutaneous spinal stimulation

Upper limb muscle-specific stimulation coincides with segmental motor pool locations

Lateral stimulation can be advantageous depending on rostral or caudal sites

Site-specific stimulation can help determine therapeutic outcomes after SCI

Oh et al., iScience 25, 105037
October 21, 2022 © 2022
https://doi.org/10.1016/j.isci.2022.105037

iScience

CellPress
OPEN ACCESS

Article

Cervical transcutaneous spinal stimulation for spinal motor mapping

Jeonghoon Oh,[1] Alexander G. Steele,[1,2] Blesson Varghese,[1] Catherine A. Martin,[1] Michelle S. Scheffler,[1] Rachel L. Markley,[1] Yi-Kai Lo,[3] and Dimitry G. Sayenko[1,4,*]

SUMMARY

Transcutaneous spinal stimulation (TSS) is a promising approach to restore upper-limb (UL) functions after spinal cord injury (SCI) in humans. We sought to demonstrate the selectivity of recruitment of individual UL motor pools during cervical TSS using different electrode placements. We demonstrated that TSS delivered over the rostrocaudal and mediolateral axes of the cervical spine resulted in a preferential activation of proximal, distal, and ipsilateral UL muscles. This was revealed by changes in motor threshold intensity, maximum amplitude, and the amount of post-activation depression of the evoked responses. We propose that an arrangement of electrodes targeting specific UL motor pools may result in superior efficacy, restoring more diverse motor activities after neurological injuries and disorders, including severe SCI.

INTRODUCTION

Neuromodulation of sensorimotor networks within the cervical and lumbosacral spinal cord via epidural (ESS) or transcutaneous (TSS) electrical spinal stimulation has been shown to have both immediate and long-term effects on motor function after spinal cord injury (SCI) (Hachmann et al., 2021; Mc Hugh et al., 2021; Taylor et al., 2021). These ESS- and TSS-induced neuromodulatory effects are achieved via physiological activation of afferents, interneurons, and projecting motor neurons resulting in an augmentative effect of spinal stimulation on voluntary motor output (Minassian and Hofstoetter, 2016; Taccola et al., 2018). Furthermore, the effects of spinal stimulation are attributed to the synergism between electrically excited neural networks and descending commands (Atkinson et al., 2022; Gerasimenko et al., 2017; Roberts et al., 2021; Steele et al., 2021). Specifically, both ESS and TSS can promote standing and stepping, as well as volitional activation of otherwise paralyzed lower-limb (LL) muscles (Angeli et al., 2018; Gill et al., 2018; Grahn et al., 2017; Rowald et al., 2022; Sayenko et al., 2019). These remarkable clinical outcomes demonstrated in LL functions have prompted several experimental trials to determine if spinal stimulation could be used to improve upper-limb (UL) function following SCI (Flores et al., 2021). While some clinical studies administering ESS and TSS have shown success in improving hand grip force (Freyvert et al., 2018; Gad et al., 2018; Inanici et al., 2018; Lu et al., 2016), limited data exist on 1) the effects of spinal stimulation therapy on other UL functions (including shoulder, elbow, and wrist flexion/extension), 2) objective electrophysiology outcomes, and 3) distinction between restorative and compensatory motor improvement following cervical spinal stimulation interventions. This decreased knowledge of the mechanisms of cervical spinal stimulation may be attributed to the difference between UL and LL descending control and biomechanics (Alstermark and Isa, 2012; Grillner, 2003; Moreno-Lopez et al., 2021; Sauerbrei et al., 2020).

In addition, anatomical differences determining feasibility of targeting specific motor pools within the lumbosacral and cervical spinal enlargements can play an important role in the success of improvement of specific UL movement patterns. Due to variation in spinal curvature and inter-rootlet anastomoses within the cervical enlargement, electrical activation of UL agonists and antagonists in a non-targeted manner can impede particular single-joint movements since the current is spread over a larger area of the cord. Furthermore, given the intrinsic complexity of cervical spinal neural networks, continuous non-patterned stimulation can excite adjacent motor pools simultaneously, irrespective of movement phase (Barra et al., 2021), and limit the efficacy of spinal neuromodulation therapy. Finally, non-targeted and non-patterned stimulation of the sensory afferents can disrupt natural movement-induced afferent inputs (Formento et al., 2018), thus hindering spinal regulation of movements that is critical for fine motor control of the UL (Barra

[1]Department of Neurosurgery, Center for Neuroregeneration, Houston Methodist Research Institute, 6550 Fannin Street, Houston, TX 77030, USA

[2]Department of Electrical and Computer Engineering, University of Houston, N308 Engineering Bldg 1, 4726 Calhoun Rd., Houston, TX 77204, USA

[3]Aneuvo, Los Angeles, CA 90024, USA

[4]Lead contact

*Correspondence: dgsayenko@houstonmethodist.org

https://doi.org/10.1016/j.isci.2022.105037

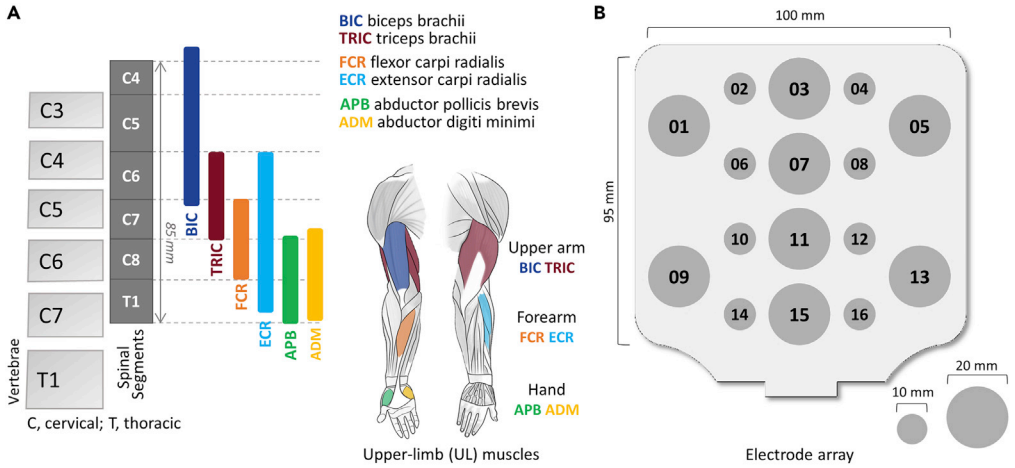

Figure 1. Cervical spinal map by epidurally evoked motor pools and cathode electrodes of transcutaneous electrical spinal stimulation

(A) Distribution of motor pools projecting to upper-limb muscles based on the segmental charts provided by (McIntyre et al., 2002). BIC: biceps brachii, TRI: triceps brachii, FCR: flexor carpi radialis, ECR: extensor carpi radialis, APB: abductor pollicis brevis, ADM: abductor digiti minimi.

(B) Electrode array with sixteen stimulation sites.

et al., 2021; Omrani et al., 2016; Sauerbrei et al., 2020). The effects of non-specific and non-patterned cervical spinal stimulation may vary after cervical SCI, depending on the lesion which can occur across different segments and impact rostrocaudal and mediolateral motor pools to different extents, including lower motoneuron lesions impacting the potential of neuromodulation interventions to regain function. Alternatively, proper and individual selection of the spinal stimulation location to target selective cervical dorsal roots and promote specific movements or functions may overcome the above-mentioned negative effects. At the same time, the extent of selectivity at different motor pools' recruitment during cervical TSS in humans remains unclear, so appropriate utilization of this selectivity may be critical for the therapeutic and functional efficacy of TSS.

The purpose of this study was to demonstrate the characteristics of TSS-evoked motor potentials using different stimulation electrodes' configurations. We characterized the recruitment patterns of different motor pools innervating UL muscles in neurologically intact individuals using TSS along the rostrocaudal and mediolateral axes of the cervical spinal enlargement (Figure 1A). We hypothesized that by using specific stimulation locations, the recruitment of individual UL motor pools will be different as revealed by motor threshold intensity, maximum amplitude, and the amount of post-activation depression. This will assist in the determination of a preferential activation of proximal versus distal, and left versus right UL muscles, based on the selective activation of the dorsal roots and motor pools. The resulting spatial activation patterns should yield an electrophysiological map that reflects the responsiveness of various motor pools projecting to the UL muscles, thus assisting in the selection of the more effective stimulation sites for facilitating performance of a given motor task.

RESULTS

Spatial patterns of activation of motor pools along the rostrocaudal axis of the cervical spinal cord

Figure 2 demonstrates the evoked responses in left BIC, FCR, and APB to double-pulse TSS delivered along the rostrocaudal axis in a representative participant. For BIC, the maximum response (MaxR) of the first response (R1) was the largest during stimulation at EL03, whereas the responses in FCR and APB were the largest at EL11. The suppression of the second response (R2) occurred in BIC and FCR during stimulation at EL03, EL07, and EL11; in APB, suppression occurred at EL07, EL11, and EL15.

Figure 3A presents the recruitment curves of all tested UL muscles during stimulation at the sites along the rostrocaudal axis. The intensity required to induce the responses increased as the stimulation site moved

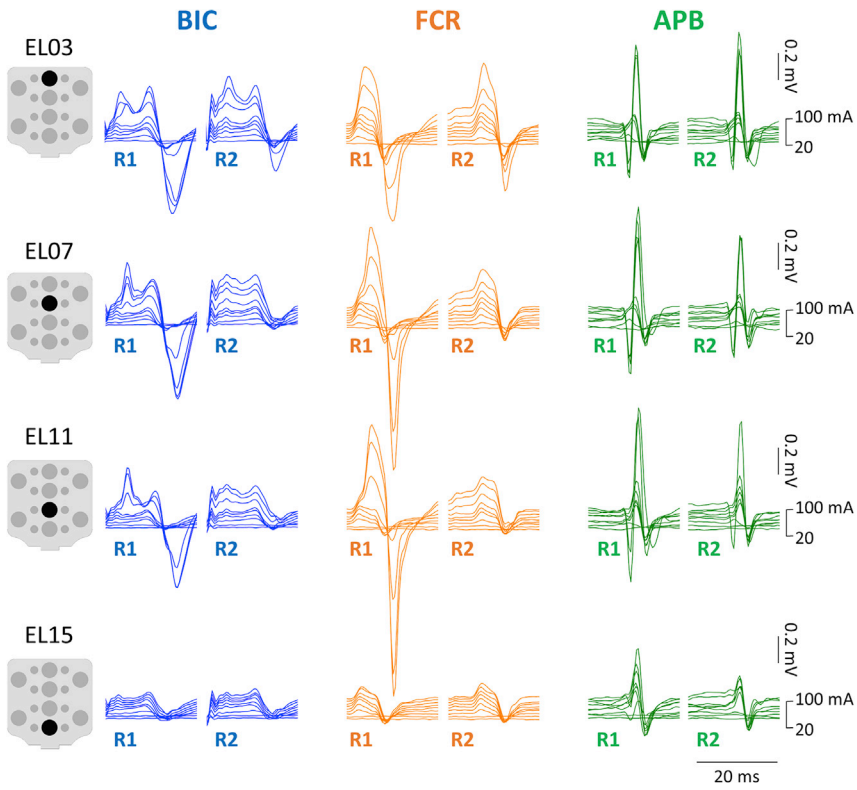

Figure 2. Examples of responses of the upper-limb muscles to double-pulse TSS along the rostrocaudal stimulation sites

The first (R1) and second responses (R2) elicited with the stimulation placed over EL03, EL07, EL11, and EL15 are shown for BIC, FCR, and APB for a representative participant (see pooled data for the R2/R1 ratio in Figure 3F). Stimulation intensity ranged from 20 to 100 mA for each site. TSS: transcutaneous spinal stimulation, BIC: biceps brachii; FCR: flexor carpi radialis; APB: abductor pollicis brevis muscles.

caudally. Specifically, the motor threshold (MT) of BIC, TRIC, and FCR was lower during stimulation at the rostral sites (EL03 and EL07) than caudal sites (EL11 and EL15). The amplitudes at rostral stimulation site at EL03 were larger for BIC, TRIC, and FCR while caudal stimulation sites at EL15 produced larger amplitudes for APB. FCR produced largest amplitude at stimulation site at EL07 and EL11.

Figure 3B shows the heatmap of the MT in the UL muscles during stimulation along the rostrocaudal axis. Our results demonstrated main effects in MT between rostrocaudal stimulation sites ($x^2(3) = 93.056$, $p < .05$). When stimulation was delivered at EL03, all listed muscles exhibited their lowest raw MT intensities ("raw" values: BIC 30.5±6.1 mA, TRIC 38.6±11.9 mA, FCR 31.4±6.0 mA, ECR 31.8±7.5 mA, APB 33.2±10.8mA, and ADM 33.6±10.0mA) with no differences in the MT among the UL muscles. At caudal sites of stimulation, MT gradually increased, with more distinct differentiation between the proximal and distal muscles. Specifically, after normalizing MT values at FCR EL07, the difference in MT first reached statistical significance between TRIC and FCR during stimulation at EL07 (TRIC 1.310±0.301, FCR = 1.0, $p < .05$) (Figure 3C). The largest MT differences between proximal and distal muscles occurred during stimulation at EL11 and EL15. There were main effects of MTs across all tested UL muscles ($\chi^2(5) = 26.648$, $p < 0.05$). Post-hoc comparisons revealed that MT was lower for BIC during stimulation at EL03 compared to the EL11 and EL15 (EL03: 0.922±0.180, EL11: 1.571±0.310, EL15: 1.874±0.399, $p < 0.001$), for TRI during stimulation at EL03 vs. EL15 (EL03: 1.161±0.323 vs. EL15: 1.755±0.366, $p < 0.01$), as well as for FCR during stimulation at EL03 (EL03: 0.942±0.111 vs. EL15: 1.504±0.262, $p < 0.01$) and EL07 (EL07 FCR = 1 vs. EL15: 1.504±0.262, $p < 0.05$) vs. EL15 (Figure 3C). The heatmap pattern and statistical analysis indicate that the stimulation over the rostral sites of the cervical spinal cord is equally effective and reveals the lowest MT for both proximal and distal UL muscle activation, whereas caudal stimulation over the cervical spinal cord is more preferential for the distal UL muscles.

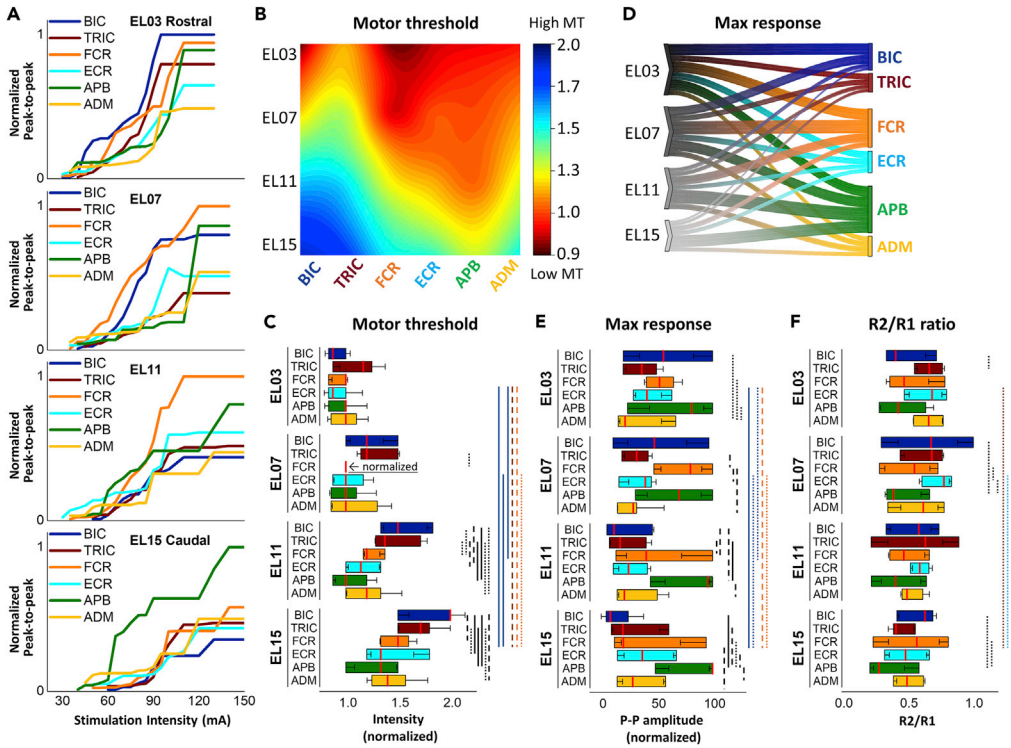

Figure 3. Responses of upper-limb muscles during TSS delivered along the rostrocaudal axis

(A) Recruitment curves of left BIC, TRIC, FCR, ECR, APB, and ADM during stimulation delivered at EL03, EL07, EL11, and EL15. Responses were normalized for each muscle using the maximum value (MaxR) across all amplitudes and sites.

(B) Heatmap of motor thresholds (MT) of the UL muscles. The MT values for each muscle were normalized to the MT of FCR at EL07.

(C) Averaged data of the MT intensity at rostrocaudal stimulation sites (see also Table S3).

(D) Parallel coordinates plots between rostrocaudal stimulation sites to the upper limb muscles derived from maximum response. Individual muscles are grouped along the right of the plot. Thickness of connections denotes the amplitude of the maximum motor response.

(E) Averaged data of the MaxR at rostrocaudal stimulation sites.

(F) Averaged data of the R2/R1 ratio at rostrocaudal stimulation sites. Box range was set as percentage 25%–75%, bold vertical red lines in boxplots present the median values, and whiskers indicate the 95% confidence interval. A post-hoc Holm-Bonferroni correction was carried out for multiple comparison within figures. Significant differences are indicated with vertical lines. Dotted lines: $p < 0.05$; dashed lines: $p < 0.01$; and solid lines: $p < 0.001$. TSS: transcutaneous spinal stimulation, BIC: biceps brachii; TRIC: triceps brachii; FCR: flexor carpi radialis; ECR: extensor carpi radialis; APB: abductor pollicis brevis; ADM: abductor digiti minimi.

Figure 3D illustrates the relationship between the rostrocaudal stimulation sites and the MaxR of the UL muscles. Stimulation at EL03 and EL07 evoked a larger response for BIC, FCR, and APB compared to more caudal stimulation sites. There were main effects of MaxR between rostrocaudal stimulation sites ($x^2(3) = 23.653$, $p < 0.001$) (Figure 3E). Post-hoc comparisons revealed that the MaxR was higher for BIC vs. ADM (BIC: 58.65±35.84 vs. ADM: 35.58±27.63, $p < 0.05$) as well as for FCR and APB vs. ADM during stimulation at EL03 (FCR: 55.9025.21, APB: 67.87±36.00, vs. ADM: 35.58±27.63, $p < 0.05$). The MaxR was higher for FCR vs. TRIC, ECR, and ADM during stimulation at EL07 (FCR: 71.97±27.22 vs. TRIC: 33.53±18.36, ECR: 37.03±18.21, ADM: 35.80±30.85, $p < 0.01$). The MaxR was higher for FCR and APB vs. BIC, TRIC, and ADM during stimulation at EL11 (FCR: 47.60±36.87, APB: 77.27±29.32 vs. BIC: 26.45±31.21, TRIC: 26.93±27.33, ADM: 38.34±33.36, $p < 0.05$), as well as for APB vs. BIC, TRIC, FCR, ECR, and ADM during stimulation at EL15 (APB: 78.85±26.89 vs. BIC: 19.17±28.18, TRIC: 31.63±31.34, FCR: 44.75±39.38, ECR: 42.88±32.92, ADM: 37.81±27.43, $p < 0.05$). In addition, there were main effects in MaxR between all tested UL muscles ($x^2(5) = 30.366$, $p < 0.001$). The MaxR of BIC was higher at EL03 compared to EL11 (EL03: 58.65±35.84 vs. EL11: 26.45±31.21, $p < 0.05$) and EL15 (EL15: 19.17±28.18, $p < 0.001$), as well as at EL07 compared to EL15 (EL07: 50.41±39.26, $p < 0.05$). The MaxR of FCR was higher

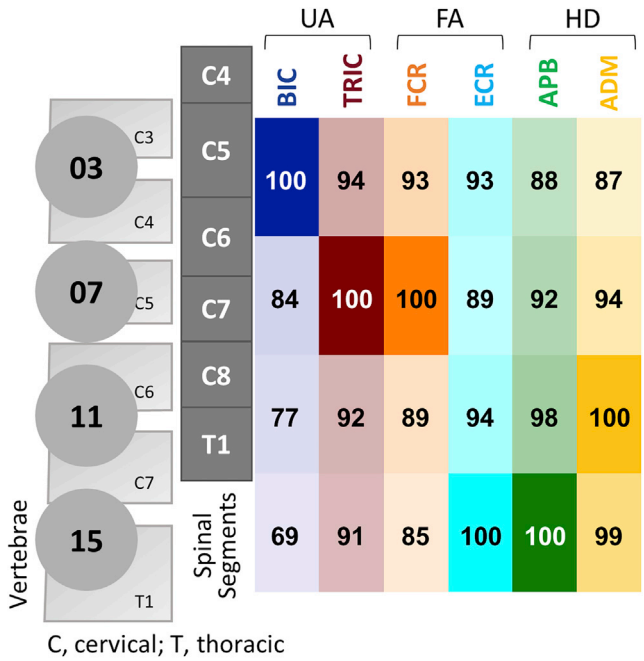

Figure 4. Probability of the upper-limb muscle response during stimulation along the rostrocaudal axis

The values in the box are calculated based on the motor threshold (MT), maximum response (MaxR), and amount of post-activation depression (R2/R1 ratio). Probabilities of muscle activation are illustrated by the opacity of different colors aligned with the stimulation electrodes. UA: upper arm; FA: forearm; HD: hand, BIC: biceps brachii; TRIC: triceps brachii; FCR: flexor carpi radialis; ECR: extensor carpi radialis; APB: abductor pollicis brevis; ADM: abductor digiti minimi.

at EL03 (EL03: 55.90±25.21 vs. EL15: 44.75±39.38, $p < 0.05$) and EL07 (EL07: 71.97±27.22, $p < 0.01$) compared to EL15. As the site of stimulation shifted caudally, the MaxR of all studied muscles except APB was reduced in amplitude ($p < 0.001$).

Analysis of the R2/R1 ratio revealed inhibition of R2 across different muscles ($\chi 2(5) = 17.560$, $p < 0.01$) (Figure 3F). The R2/R1 ratio was lower for BIC compared to TRIC during stimulation at EL03 (BIC: 0.493±0.223, TRIC: 0.683±0.155, $p < 0.05$). The R2/R1 ratio was lower for APB compared to BIC and ECR, and for FCR vs. ECR at EL07 (BIC: 0.661±0.340, FCR: 0.503±0.258, ECR: 0.711±0.172, APB: 0.470±0.206, $p < 0.05$) as well as for ABP vs. BIC and FCR at EL15 (BIC: 0.583±0.217, FCR: 0.554±0.289, APB: 0.363±0.178, $p < 0.05$). Post-hoc comparisons revealed that the R2/R1 ratio was lower for TRIC during stimulation at EL15 compared to EL03 (EL15: 0.455 ± 0.146, EL03: 0.683 ± 0.155), as well as for ECR during stimulation at EL15 than EL07 (EL15: 0.507 ± 0.212 vs. EL07: 0.711 ± 0.172). Statistical analysis showed the effects of the electrode position on the R2/R1 ratio in individual muscles; however, there was no significant difference between proximal and distal muscles.

Figure 4 shows the probability of activation of motor pools projecting to proximal and distal UL muscles during stimulation along the rostrocaudal axis. The probability of activation of BIC was the highest at EL03. TRIC and FCR at EL07, ECR and APB at EL15, ADM at EL11.

Spatial patterns of activation of motor pools along the mediolateral axis of the cervical spinal cord

Figure 5 exemplifies the evoked responses in left and right BIC, FCR, and APB to double-pulse TSS delivered at the lateral (EL01 and EL09) and midline (EL03 and EL11) sites in a representative participant. During stimulation at EL01, larger responses were observed in BIC and APB, whereas the responses in FCR did not demonstrate clear relationship with the ipsilateral vs. midline stimulation. During stimulation at EL09, the larger responses were observed in APB, whereas the responses in BIC and FCR did not demonstrate clear relationship with the ipsilateral vs. midline stimulation. In this example, the R2 in contralateral BIC and FCR

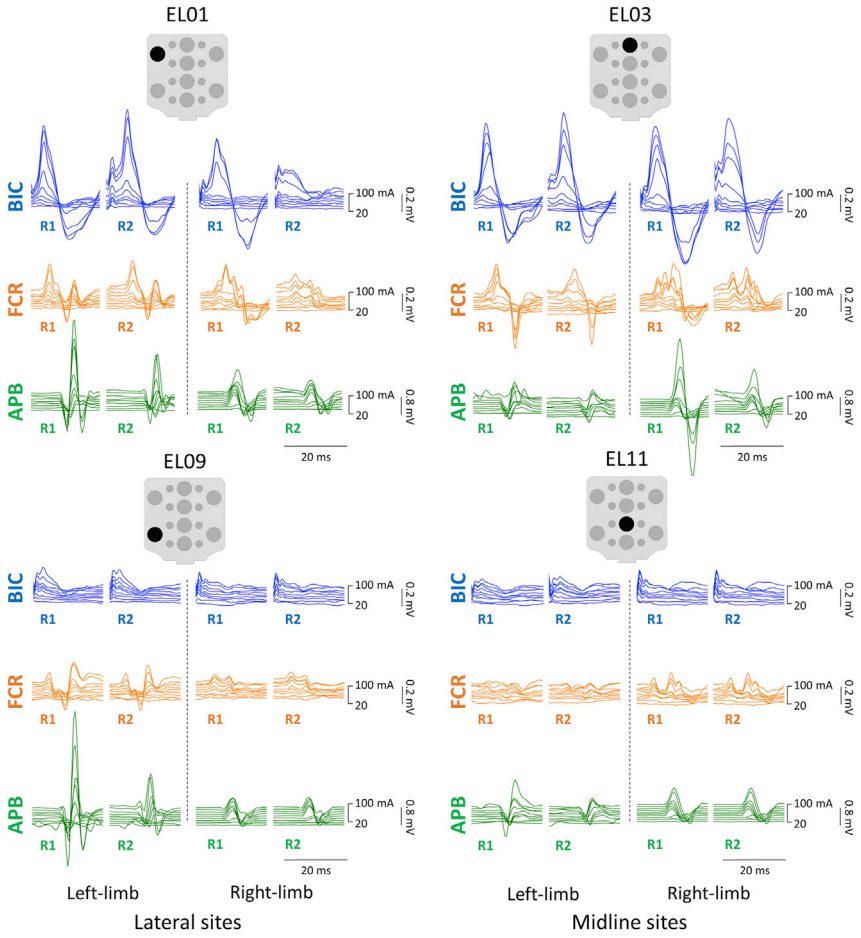

Figure 5. Examples of responses of the left and right upper-limb muscles to double-pulse TSS at lateral (EL01 and EL09) and midline stimulation sites (EL03 and EL11)

The first (R1) and second responses (R2) elicited with the stimulation placed each electrode are shown for BIC, FCR, and APB for a representative participant. Stimulation intensity ranged from 20 to 100 mA for each site. TSS: transcutaneous spinal stimulation, BIC: biceps brachii; FCR: flexor carpi radialis; APB: abductor pollicis brevis muscles.

was suppressed during stimulation at EL01 but not at EL03; whereas in ipsilateral APB the R2 was suppressed during stimulation at EL01 and EL09 but not at EL03 and EL11 for an exemplary participant.

Figure 6 demonstrates the relationship between stimulation at the ipsi- and contralateral sites at the rostral and caudal cervical spinal cord. Preferential activation of BIC and FCR was evident during ipsilateral stimulation at rostral lateral sites and during stimulation over the midline at caudal sites. APB demonstrated preferential activation during stimulation at both rostral and caudal ipsilateral sites.

Figure 7 shows the analysis of the MT, MaxR, and R2/R1 ratio during stimulation over the lateral (EL01, EL05, EL09, and EL13), mid-lateral (EL02, EL04, EL10, and EL12), and midline (EL03 and EL11) sites. There were main effects of MTs across all tested UL muscles at rostral ($\chi 2(5) = 39.109$, $p < 0.001$) and caudal mediolateral sites ($\chi 2(5) = 113.084$, $p < 0.001$) (Figures 7A and 7B). Post-hoc comparisons revealed that the MT was higher for BIC during stimulation at EL01 compared to the EL03 (EL01: 1.27 ± 0.29, EL03: 0.92 ± 0.17, $p < 0.05$). The MT was higher for TRIC vs. FCR and ECR during stimulation at EL01, for TRIC vs. FCR, ECR, and APB, as well as for BIC vs. ECR during stimulation at EL04. Post-hoc comparisons revealed that the MTs were consistently lower for FCR, ECR, APB, and ADM, as compared to those in BIC and TRIC during stimulation at caudal mediolateral sites. The effects of the site of stimulation revealed the difference in BIC during stimulation via lateral (EL09 and EL13) vs. midline (EL11) sites (EL09: 2.186 ± 0.726, EL11: 1.571 ± 0.296, EL13: 2.217 ± 0.917, $p < 0.001$).

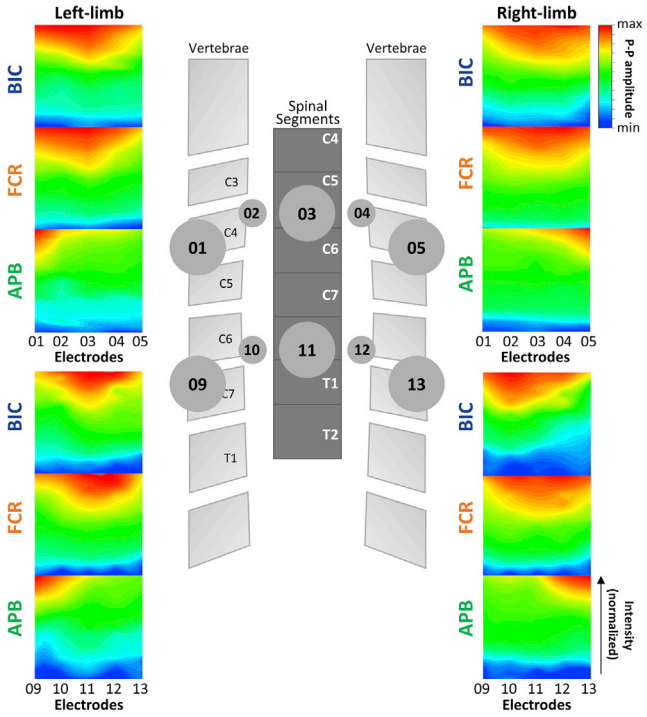

Figure 6. Ipsilateral upper-limb muscle activation during TSS delivered along the mediolateral axis of the cervical spinal cord

Heatmap pattern of motor evoked responses with ipsilateral versus contralateral stimulation sites using normalized MaxR for left and right BIC, FCR, and APB for the rostral mediolateral (EL01, EL02, EL03, EL04, and EL05) and caudal mediolateral (EL09, EL10, EL11, EL12, and EL13) stimulation sties.

There were main effects of MaxR across all tested UL muscles at rostral ($\chi 2(5) = 42.012$, $p < 0.001$) and caudal mediolateral sites ($\chi 2(5) = 90.811$, $p < 0.001$) (Figures 3C and 3D). During stimulation via both rostral and caudal lateral sites (EL01, EL05, EL09, EL10, EL12, and EL13), APB produced larger MaxR as compared to the other muscles (Figures 7C and 7D). The effects of lateral vs. midline sites were found in APB during both rostral (EL01: 258.27 ± 193.42, $p < 0.01$; EL05: 270.65 ± 210.23, $p < 0.001$) (Figure 7C) and caudal mediolateral sites (EL09: 336.99 ± 435.75, $p < 0.05$; EL13: 438.99 ± 600.54, $p < 0.001$) as well as lower MaxR in FCR during rostral sites at EL01 (FCR: 86.338 ± 48.997, $p < 0.05$) (Figure 7D).

There were main effects of inhibition of R2 across all tested UL muscles at rostral ($\chi 2(5) = 20.330$, $p < 0.01$) and caudal ($\chi 2(5) = 30.594$, $p < 0.001$) mediolateral sites. For the rostral mediolateral sites (Figure 7E), the R2/R1 ratio was lower for BIC compared to TRIC during stimulation at EL02 (BIC: 0.488 ± 0.295 vs. TRIC: 0.714 ± 0.152, $p < 0.05$), as well as for BIC vs. ECR and ADM at EL04 (BIC: 0.421 ± 0.217 vs. ECR: 0.664 ± 0.157, ADM: 0.679 ± 0.240, $p < 0.05$). The R2/R1 ratio was lower for APB compared to TRIC, ECR and ADM at EL01 (APB: 0.419 ± 0.209 vs. TRIC: 0.614 ± 0.245, ECR: 0.609 ± 0.152, ADM: 0.610 ± 0.231, $p < 0.05$), and for APB vs. ECR at EL02 (APB: 0.537 ± 0.239 vs. ECR: 0.755 ± 0.157, $p < 0.05$). The R2/R1 ratio of FCR was lower at EL03 compared to EL05 (EL03: 0.456 ± 0.223 vs. EL05: 0.656 ± 0.204, $p < 0.05$) and of ECR at EL05 vs. EL02 (EL05: 0.521 ± 0.216 vs. EL02: 0.755 ± 0.157, $p < 0.05$). For the caudal mediolateral sites (Figure 7F), the R2/R1 ratio was lowered for ECR compared to BIC and TRIC at EL09, for APB vs. BIC, TRIC and ADM at EL09, and BIC, TRIC, and ECR at EL10, for ADM vs. BIC, TRIC, and ECR at EL10, as well as for APB and ADM vs. TRIC at EL12. The R2/R1 ratio of ECR was lowered at EL09 compared to EL10 (EL09: 0.443 ± 0.130 vs. EL10: 0.630 ± 0.226, $p < 0.05$).

Figure 8 shows the probability of activation of the UL motor pools during stimulation along the rostral and caudal mediolateral axes. During stimulation at rostral mediolateral sites, probability of activation of BIC was the highest at the midline site (EL03), TRIC, FCR, ECR, and APB—at mid-lateral sites, ADM—at lateral site (Figure 8A). During stimulation at caudal mediolateral sites, probability of activation of BIC, TRIC, and

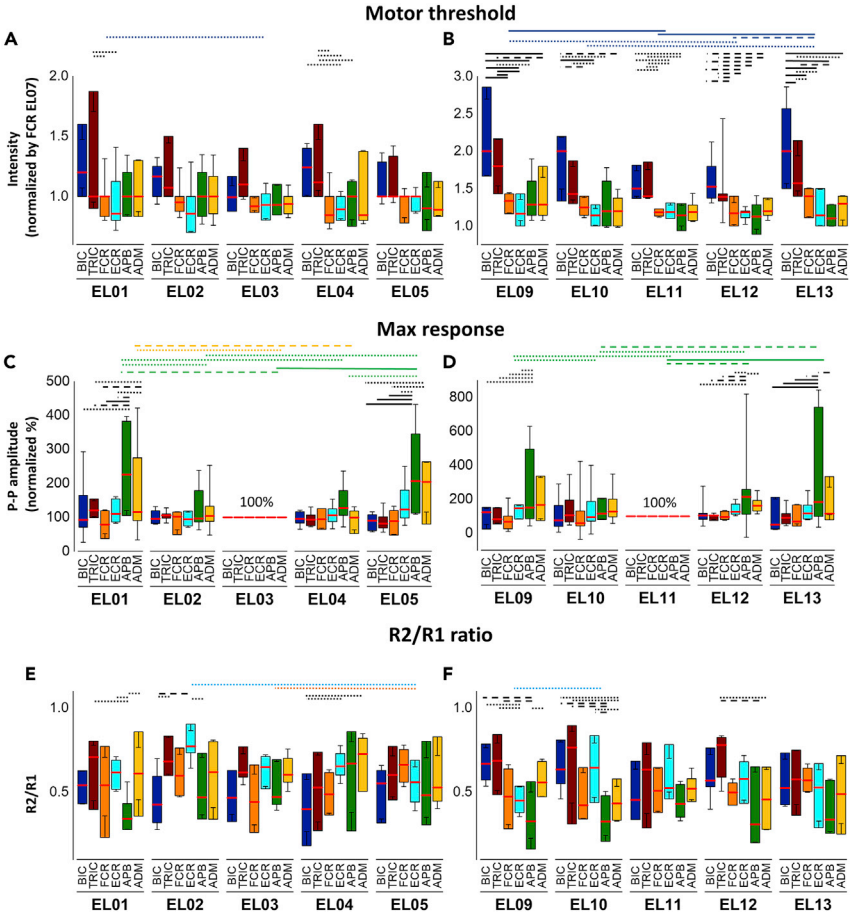

Figure 7. Statistical comparison between six of upper-limb muscles during TSS delivered along the mediolateral axes

(A) Averaged data of the MT intensity at rostral mediolateral stimulation sites (see also Table S3).

(B) Averaged data of the MT at caudal mediolateral stimulation sites (see also Table S3).

(C) Averaged data of the MaxR at rostral mediolateral stimulation sites.

(D) Averaged data of the MaxR at caudal mediolateral stimulation sites.

(E) Averaged data of the R2/R1 ratio at rostral mediolateral stimulation sites.

(F) Averaged data of the R2/R1 ratio at caudal mediolateral stimulation sites. Box range was set as percentage 25%–75%, bold horizontal red lines in boxplots present the median values, and whiskers indicate the 95% confidence interval. A post-hoc Holm-Bonferroni correction was carried out for multiple comparison within figures. Significant differences are indicated with horizontal lines. Dotted lines: $p < 0.05$; dashed lines: $p < 0.01$; and solid lines: $p < 0.001$. Rostral mediolateral stimulation sites include EL01, EL02, EL03, EL4, and EL05; caudal mediolateral stimulation sites include EL09, EL10, EL11, EL12, and EL13. TSS: transcutaneous spinal stimulation, BIC: biceps brachii; TRIC: triceps brachii; FCR: flexor carpi radialis; ECR: extensor carpi radialis; APB: abductor pollicis brevis; ADM: abductor digiti minimi.

FCR was the highest at the midline site (EL11), ECR, and APB—at lateral sites, ADM—mid-lateral site (Figure 8B).

DISCUSSION

This study demonstrated that TSS delivered over the rostral and caudal, as well as midline and lateral aspects of the cervical spinal cord resulted in preferential activation of proximal, distal, and ipsilateral UL muscles, revealed by changes in motor threshold intensity, maximum amplitude, and the amount of post-activation depression of the evoked responses. While rostral stimulation resulted in activation of all tested muscles (except APB) generating a large magnitude of response, caudal stimulation produced a larger magnitude of response at distal muscles. A similar comparison was observed with stimulation along

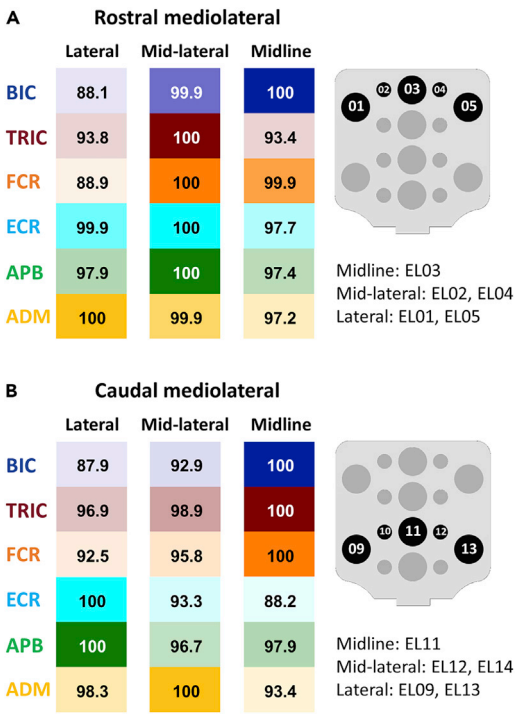

Figure 8. Probability of the upper-limb muscle response during stimulation along the mediolateral axes

(A) Probability of motor response for BIC, TRI, FCR, ECR, APB, and ADM at rostral mediolateral stimulation site. Stimulation via lateral (EL01 and EL05), mid-lateral (EL02 and EL04), and midline (EL03) portion of array was averaged.

(B) Probability of motor response for BIC, TRI, FCR, ECR, APB, and ADM at each caudal mediolateral stimulation site. Stimulation via lateral (EL09 and EL13), mid-lateral (EL10 and EL12), and midline (EL13) portion of array was averaged.

the mediolateral axis. Midline stimulation resulted in a higher probability of activation at proximal muscles, and stimulation at lateral sites resulted in a higher probability of activation at distal muscles.

TSS delivered along the rostrocaudal axis of the cervical spinal cord results in preferential activation of proximal and distal UL muscles

Studies with lumbar spinal stimulation have demonstrated that both ESS and TSS administered based on the anatomical maps of the spinal cord can selectively engage specific motoneurons projecting to the LL muscles (Sayenko et al., 2014, 2015). Specifically, stimulation of rostral and caudal areas of the lumbar spinal cord resulted in a relatively selective activation of proximal and distal LL motor pools. Furthermore, stimulation via a set of electrodes localized over specific spinal segments allowed for selective recruitment of the motor pools, whereas a wide-field stimulation resulted in a generalized pattern of activation of proximal and distal motor pools. Previous work on mapping the lumbosacral spinal cord using ESS based on the relative motor threshold values for proximal and distal muscles indicates rostrocaudal spatial dispersions of the respective motor pools (Hofstoetter et al., 2021). Our work demonstrates that a similar approach can be utilized to map cervical spinal motor pools using TSS. At the same time, exclusive activation of LL agonist muscles without concomitant involvement of their antagonists during lumbar spinal stimulation is still challenging and was reported only in a subset of works using ESS (Rowald et al., 2022; Wagner et al., 2018).

Cervical ESS along the rostrocaudal axis was recently investigated in primates (Barra et al., 2021; Greiner et al., 2021; Guiho et al., 2021; Kato et al., 2020). Similar to the lumbar ESS, the recruitment patterns of UL muscles corresponded to the rostrocaudal innervation of motor nuclei. While individual activation of the upper arm antagonists (i.e., BIC and TRIC) was achieved in these experiments, selective activation of forearm and hand muscles was challenging, likely due to the overlapping innervation of forearm and hand muscles (Greiner et al., 2021).

There are limited reports describing the responses to cervical TSS at different spinal levels along the rostrocaudal axis. de Freitas et al. (2021) attempted to address the relative effects of activation of sensory and motor pathways using different placement of stimulation and reference electrodes. They demonstrated that motor pools projected to the hand muscles were preferentially activated when the cathode was placed over T1 compared with rostral vertebral levels, whereas there was no selectivity for motor pools projected

to proximal UL muscles. Furthermore, higher stimulation intensities were required to activate distal than proximal UL muscles, suggesting different excitability thresholds between UL motor pools (de Freitas et al., 2021).

Our data are consistent with previous reports, as well as with the anatomy and myotomal maps of the cervical spinal cord (Figure 1A). We found that TSS delivered within a relatively narrow range between the C3 and T1 vertebrae resulted in a different order of activation and magnitude of recruitment of the proximal and distal motor pools. At each location used, the stimulation always activated both proximal and distal UL muscles. However, the intensity required to activate different UL motor pools, the relative order of recruitment of different UL muscles, and the maximum magnitude of their responses were dependent on the site of stimulation. Stimulation over the rostral sites corresponding to C4 and C5 vertebrae required lower intensities to activate the UL motor pools, with little to no difference in the order of their recruitment. The magnitude of responses at these locations was larger in all tested muscles but APB. During stimulation at more caudal sites corresponding to C6 and T1 vertebrae, higher intensities were required, and more pronounced differences were observed in the order of activation between proximal and distal motor pools. We also demonstrated relative selectivity in activation of the upper arm (BIC and TRIC) and forearm (FCR and ECR) agonist and antagonist muscles.

Our findings during cervical stimulation contrast previous observations during lumbar TSS when stimulation over the caudal portions was associated with lower MT intensities and larger magnitude of the induced muscle responses. Anatomical similarities of the rostral cervical and caudal lumbar spinal cord, such as the curvature and proximity of dorsal roots to the surface, as well as the number of dorsal and ventral rootlets, can explain these observations (Mendez et al., 2020). However, the primary factor is likely the compact arrangement of the UL motor pools and inter-rootlet anastomoses (Mendez et al., 2020). Thus, non-invasive stimulation directly over the cervical enlargement activates all UL motor pools and with lower thresholds. However, preferential activation of caudal UL motor pools can be achieved by stimulating caudal to the cervical enlargement.

TSS delivered along the mediolateral axis of the cervical spinal cord results in preferential activation of ipsilateral UL muscles

Recent data obtained using cervical ESS in primates indicate that near full and exclusive recruitment of individual roots can be achieved with lateral electrodes (Barra et al., 2021; Greiner et al., 2021). In particular, the amplitude of muscle activation and muscle recruitment specificity were higher with lateral compared to midline stimulation (Greiner et al., 2021). Based on experimental and simulation data, the authors suggested that laterally positioned electrodes can recruit Ia afferents of a targeted root at stimulation amplitudes that are subthreshold for the afferents residing in other roots. However, with increased stimulation amplitude, the concomitant recruitment of afferents of nontargeted roots is likely to occur. Thus, higher stimulation amplitudes may recruit fibers coming from roots not specific to the stimulation site. We demonstrated a difference in activation of ipsilateral and contralateral motor pools during stimulation using rostral and caudal lateral electrodes. The most pronounced activation of upper arm and forearm muscles was observed during rostral lateral stimulation. Hand muscles showed preferential activation during stimulation at both rostral and caudal lateral sites. When stimulating at midline site, BIC had the highest probability of activation rostrally and caudally. TRIC mirrored this pattern, with an additional highest probability of activation at the rostral mid-lateral site. Forearm muscles demonstrated a more balanced probability of activation with regards to location sites. Specifically, FCR followed with highest probability of activation at mid-lateral sites when stimulating rostrally, but at midline sites when stimulating caudally. ECR, however, began to differentiate slightly. Like FCR, ECR had the highest probability of activation at the mid-lateral site when stimulating rostrally, but when stimulating caudally, the highest probability of activation shifted laterally. For the hand muscles, the highest probability of activation was at mid-lateral and lateral sites both rostrally and caudally. These findings support our conclusions that administration of site-specific cervical TSS can target specific UL motor pools based on location of administration. We did not observe the advantageous effects of lateral stimulation on the maximum amplitude of the evoked responses or specificity on targeting individual motor pools, as demonstrated using cervical ESS in primates (Barra et al., 2021; Greiner et al., 2021). This can be attributed to the localized nature of electrical field generated via much smaller epidural electrodes (i.e., 1 to 1.5 mm) located closer to the dorsal roots, as opposed to the larger (i.e., 1 to 2 cm) surface electrodes transmitting a wide-field current and causing generalized activation of the afferents within neighboring dorsal roots. It is worth noting that we did not observe considerable changes in

the R2/R1 ratio between the lateral and midline stimulation sites, which indicates similar involvement of the sensory and motor pathways. From a practical perspective, stimulation via lateral electrodes may also activate adjacent upper back muscles (e.g., trapezius) to a larger extent than during midline stimulation, thus potentially affecting the resultant UL movements. Therefore, administration of lateral cervical TSS should be weighted between the goal of specific ipsilateral UL muscle activation and expected movement kinematics.

Cervical TSS engages both sensory and motor pathways

Spinal stimulation delivered over the cervical and lumbar spinal cord may excite the sensory and motor pathways to different extents. The engagement of each pathway seems critical for the effects and for understanding the mechanisms of spinal stimulation therapy. Specifically, activation of sensory fibers lying in the dorsal roots and synapsing on motoneurons projecting to the limb muscles would interface with spinal interneurons as well as intraspinal ascending and descending connections (Atkinson et al., 2022; Sayenko et al., 2014). This can contribute to stimulation-induced changes within the spinal and supraspinal sensorimotor networks (Manson et al., 2022). In our previous studies with ESS and TSS over the lumbar spinal cord, we demonstrated the modulatory effects of the stimulation frequency, intensity, and sensory feedback on spinally evoked potentials (Sayenko et al., 2014, 2015). This reveals the transsynaptic route of the underlying motoneuronal recruitment via the afferent activation within the dorsal roots. Functional and clinical effects of this mechanism were evident in previous studies using spinal stimulation (Hachmann et al., 2021; Taylor et al., 2021). Alternatively, stimulation of motor axons residing in the ventral roots would result in postsynaptic activation of the neuromuscular junction, producing muscle contractions yet bypassing spinal circuits. These induced responses are not susceptive to modulation, and their effects on sensorimotor network reorganization can be minimal.

Furthermore, we sought to investigate whether sensory and motor activation depends on the site of stimulation over the cervical spinal cord. We found that double-pulse TSS attenuated the second evoked motor responses (R2) in the pairs, suggesting the transsynaptic nature of the underlying motoneuronal recruitment. However, the fact that the R2s were not fully suppressed demonstrating an inevitable direct recruitment of motor axons. There were differences in the R2 suppression (e.g., for TRIC and ECR at the rostrocaudal sites, and FCR and ECR at the mediolateral sites), albeit for most muscles the R2 suppression did not depend on the stimulation site. Our observations, although supporting the feasibility of cervical TSS to engage spinal sensorimotor networks via the dorsal roots, also indicate the challenge of selective recruitment of sensory routes, even if the stimulation is delivered at different sites of the cervical spinal cord. This is not surprising given the compact anatomy of the UL motor pools in the cervical enlargement, adjacent layout of dorsal and ventral roots, inter-rootlet anastomoses, and proximity of the stimulation sites to the brachial plexus. For clinical applications, TSS intensity may need to be individually adjusted at a given stimulation location to yield the highest R2 suppression, thus ensuring the most optimal stimulation parameters for targeting the sensory route. Future work should also look at the effect of inter-stimulus interval to systematically investigate the refractory period of spinal motor pools in UL muscles.

Clinical implications

The present findings should be implemented acknowledging potential inter-individual variability of the anatomical relationship between the cervical spinal cord and vertebrae as well as differences in the segmental myotomal charts of UL motor pools. We suggest that the vertebral levels presented in our study will be used as approximate guidance, and the exact spatiotemporal maps of the proximal and distal UL muscles should be determined individually during TSS over the cervical spinal cord, using the recruitment characteristics described. In addition, variations in threshold and magnitude of evoked potentials among different individuals can result from anatomical differences in underlying skin resistance, amounts of subcutaneous fat, muscle tone, density of vertebral bone, intervertebral space and ligaments, as well as implanted hardware. Because the electrical conductivity of implanted hardware differs from that of the surrounding tissue, current flow is altered and therefore needs to be taken into account when applying TSS.

In clinical populations, the level and extent of SCI can affect the response of activated motor pools. While for restoration of lower limb functions, lumbar spinal stimulation is conventionally applied several vertebral levels below the lesion, the proximity of the injury and targeted neural structures in the cervical spinal

cord can confound the spatial map of the evoked responses. Rostrocaudal and mediolateral specificity of activation of the proximal, distal, and ipsilateral UL motor pools in individuals with cervical SCI can be affected not only by the site of stimulation but also by whether the activated motoneurons are located above, below, or over the lesion. As such, the resultant spatial map obtained from the assessment of evoked potentials above and below the lesion would contribute to the comprehensive understanding of the viability and function of selected UL motor pools. In turn, this may dictate individually adjusted cervical TSS administration. It is a question for further research whether stimulation must be delivered to engage "more fragile" or "more viable" motor pools to "revive" or "build on" their function, respectively, and will most likely depend on the individual function. Regardless, preferential activation of the UL motor pools following neurorehabilitation interventions after SCI would allow researchers and clinicians to monitor changes in their recruitment patterns.

Finally, characteristics of spinal reflexes highly depend on the descending and segmental conditions, the level of muscle activity, and the task performed (Atkinson et al., 2022; Milosevic et al., 2019; Pierrot-Deseilligny and Burke, 2005; Steele et al., 2021). Although we demonstrated the spatial effects of TSS on the cervical sensorimotor networks, there is a need to investigate to what extent the spinal segment-specific effects obtained in a resting state are relevant during different motor tasks, including rehabilitation of UL function.

In conclusion, we have demonstrated the relationship between the rostrocaudal and mediolateral sites of cervical TSS and characteristics of spinally evoked motor potentials in the UL muscles. TSS delivered over the rostral and caudal as well as midline and lateral aspects of the cervical spine resulted in a preferential activation of proximal, distal, and ipsilateral UL muscles, as evidenced by changes in motor threshold intensity, maximum amplitude, and the amount of post-activation depression of the evoked responses. Our findings provide a baseline for future clinical trials in people with neurological injuries, including people with cervical SCI, for mapping motor pools with the goal of restoring function targeting specific UL motor pools.

Limitations of the study

The neck height and circumferences of the participants were not taken into account, despite their importance in determining the precise rostrocaudal and mediolateral placement of electrodes. In addition, as responses were only recorded on the left side during rostrocaudal stimulation, hand dominance may have influenced the motor responses. Lastly, variations in threshold and magnitude of the evoked potential among different individuals can result from difference in the underlying skin resistance, amounts of subcutaneous fat, size of muscles, vertebral bone, and intervertebral ligaments.

STAR★METHODS

Detailed methods are provided in the online version of this paper and include the following:

- KEY RESOURCES TABLE
- RESOURCE AVAILABILITY
  - Lead contact
  - Materials availability
  - Data and code availability
- EXPERIMENTAL MODEL AND SUBJECT DETAILS
  - Human subjects
- METHOD DETAILS
  - Cervical transcutaneous spinal stimulation
  - EMG recording and data collection
  - Data processing and analysis
  - Motor activation patterns of rostrocaudal and mediolateral stimulation sites
  - Probability of motor activation
- QUANTIFICATION AND STATISTICAL ANALYSIS

SUPPLEMENTAL INFORMATION

Supplemental information can be found online at https://doi.org/10.1016/j.isci.2022.105037.

ACKNOWLEDGMENTS

This work was in part supported by the NeuroSpark Seed Funding Program (20130009) and Craig H. Neilsen Foundation (733278). The multi-electrode arrays were provided by Aneuvo.

AUTHOR CONTRIBUTIONS

Conceptualization, D.G.S.; Data curation, J.O., A.G.S., B.V., R.L.M., and D.G.S.; Formal analysis, J.O. and D.G.S.; Funding acquisition, D.G.S.; Investigation, D.G.S.; Methodology, J.O., Y.-K.L., and D.G.S.; Supervision, D.G.S.; Visualization, J.O., A.G.S., and D.G.S.; Writing—original draft, J.O., A.G.S., and D.G.S.; Writing—review & editing, J.O., A.G.S., C.A.M., M.S.S., R.L.M., Y.-K.L., and D.G.S.

DECLARATION OF INTERESTS

Y.-K.L. holds shareholder interest in Aneuvo.

Received: April 13, 2022
Revised: July 29, 2022
Accepted: August 25, 2022
Published: October 21, 2022

REFERENCES

Alstermark, B., and Isa, T. (2012). Circuits for skilled reaching and grasping. Annu. Rev. Neurosci. *35*, 559–578.

Andrews, J.C., Stein, R.B., and Roy, F.D. (2015). Post-activation depression in the human soleus muscle using peripheral nerve and transcutaneous spinal stimulation. Neurosci. Lett. *589*, 144–149.

Angeli, C.A., Boakye, M., Morton, R.A., Vogt, J., Benton, K., Chen, Y., Ferreira, C.K., and Harkema, S.J. (2018). Recovery of over-ground walking after chronic motor complete spinal cord injury. N. Engl. J. Med. *379*, 1244–1250.

Atkinson, D.A., Steele, A.G., Manson, G.A., Sheynin, J., Oh, J., Gerasimenko, Y.P., and Sayenko, D.G. (2022). Characterization of interlimb interaction via transcutaneous spinal stimulation of cervical and lumbar spinal enlargements. J. Neurophysiol. *127*, 1075–1085.

Barra, B., Conti, S., Perich, M.G., Zhuang, K., Schiavone, G., Fallegger, F., Galan, K., James, N.D., Barraud, Q., Delacombaz, M., et al. (2021). Epidural electrical stimulation of the cervical dorsal roots restores voluntary arm control in paralyzed monkeys. Preprint at bioRxiv. https://doi.org/10.1101/2020.11.13.379750.

Calvert, J.S., Manson, G.A., Grahn, P.J., and Sayenko, D.G. (2019). Preferential activation of spinal sensorimotor networks via lateralized transcutaneous spinal stimulation in neurologically intact humans. J. Neurophysiol. *122*, 2111–2118.

de Freitas, R.M., Sasaki, A., Sayenko, D.G., Masugi, Y., Nomura, T., Nakazawa, K., and Milosevic, M. (2021). Selectivity and excitability of upper-limb muscle activation during cervical transcutaneous spinal cord stimulation in humans. J. Appl. Physiol. *131*, 746–759.

Flores, Á., López-Santos, D., and García-Alías, G. (2021). When spinal neuromodulation meets sensorimotor rehabilitation: lessons learned from animal models to regain manual dexterity after a spinal cord injury. Front. Rehabil. Sci. *2*.

Formento, E., Minassian, K., Wagner, F., Mignardot, J.B., Le Goff-Mignardot, C.G., Rowald, A., Bloch, J., Micera, S., Capogrosso, M., and Courtine, G. (2018). Electrical spinal cord stimulation must preserve proprioception to enable locomotion in humans with spinal cord injury. Nat. Neurosci. *21*, 1728–1741.

Freyvert, Y., Yong, N.A., Morikawa, E., Zdunowski, S., Sarino, M.E., Gerasimenko, Y., Edgerton, V.R., and Lu, D.C. (2018). Engaging cervical spinal circuitry with non-invasive spinal stimulation and buspirone to restore hand function in chronic motor complete patients. Sci. Rep. *8*, 15546.

Gad, P., Lee, S., Terrafranca, N., Zhong, H., Turner, A., Gerasimenko, Y., and Edgerton, V.R. (2018). Noninvasive activation of cervical spinal networks after severe paralysis. J. Neurotrauma *35*, 2145–2158.

Gerasimenko, Y., Sayenko, D., Gad, P., Liu, C.T., Tillakaratne, N.J.K., Roy, R.R., Kozlovskaya, I., and Edgerton, V.R. (2017). Feed-forwardness of spinal networks in posture and locomotion. Neuroscientist *23*, 441–453.

Gill, M.L., Grahn, P.J., Calvert, J.S., Linde, M.B., Lavrov, I.A., Strommen, J.A., Beck, L.A., Sayenko, D.G., Van Straaten, M.G., Drubach, D.I., et al. (2018). Neuromodulation of lumbosacral spinal networks enables independent stepping after complete paraplegia. Nat. Med. *24*, 1677–1682.

Grahn, P.J., Lavrov, I.A., Sayenko, D.G., Van Straaten, M.G., Gill, M.L., Strommen, J.A., Calvert, J.S., Drubach, D.I., Beck, L.A., Linde, M.B., et al. (2017). Enabling task-specific volitional motor functions via spinal cord neuromodulation in a human with paraplegia. Mayo Clin. Proc. *92*, 544–554.

Greiner, N., Barra, B., Schiavone, G., Lorach, H., James, N., Conti, S., Kaeser, M., Fallegger, F., Borgognon, S., Lacour, S., et al. (2021). Recruitment of upper-limb motoneurons with epidural electrical stimulation of the cervical spinal cord. Nat. Commun. *12*, 435.

Grillner, S. (2003). The motor infrastructure: from ion channels to neuronal networks. Nat. Rev. Neurosci. *4*, 573–586.

Guiho, T., Baker, S.N., and Jackson, A. (2021). Epidural and transcutaneous spinal cord stimulation facilitates descending inputs to upper-limb motoneurons in monkeys. J. Neural. Eng. *18*, 046011.

Hachmann, J.T., Yousak, A., Wallner, J.J., Gad, P.N., Edgerton, V.R., and Gorgey, A.S. (2021). Epidural spinal cord stimulation as an intervention for motor recovery after motor complete spinal cord injury. J. Neurophysiol. *126*, 1843–1859.

Hofstoetter, U.S., Freundl, B., Danner, S.M., Krenn, M.J., Mayr, W., Binder, H., and Minassian, K. (2020). Transcutaneous spinal cord stimulation induces temporary attenuation of spasticity in individuals with spinal cord injury. J. Neurotrauma *37*, 481–493.

Hofstoetter, U.S., Perret, I., Bayart, A., Lackner, P., Binder, H., Freundl, B., and Minassian, K. (2021). Spinal motor mapping by epidural stimulation of lumbosacral posterior roots in humans. iScience *24*, 101930.

Inanici, F., Samejima, S., Gad, P., Edgerton, V.R., Hofstetter, C.P., and Moritz, C.T. (2018). Transcutaneous electrical spinal stimulation promotes long-term recovery of upper extremity function in chronic tetraplegia. IEEE Trans. Neural Syst. Rehabil. Eng. *26*, 1272–1278.

Kato, K., Nishihara, Y., and Nishimura, Y. (2020). Stimulus outputs induced by subdural electrodes on the cervical spinal cord in monkeys. J. Neural. Eng. *17*, 016044.

Lu, D.C., Edgerton, V.R., Modaber, M., AuYong, N., Morikawa, E., Zdunowski, S., Sarino, M.E., Sarrafzadeh, M., Nuwer, M.R., Roy, R.R., and Gerasimenko, Y. (2016). Engaging cervical spinal cord networks to reenable volitional control of hand function in tetraplegic patients. Neurorehabil. Neural Repair *30*, 951–962.

Manson, G.A., Atkinson, D.A., Shi, Z., Sheynin, J., Karmonik, C., Markley, R.L., and Sayenko, D.G. (2022). Transcutaneous spinal stimulation alters cortical and subcortical activation patterns during mimicked-standing: a proof-of-concept fMRI study. Neuroimage: Reports *2*, 100090.

Mc Hugh, C., Taylor, C., Mockler, D., and Fleming, N. (2021). Epidural spinal cord stimulation for motor recovery in spinal cord injury: A systematic review. NeuroRehabilitation, 1–24.

McIntyre, C.C., Richardson, A.G., and Grill, W.M. (2002). Modeling the excitability of mammalian nerve fibers: influence of afterpotentials on the recovery cycle. J. Neurophysiol. *87*, 995–1006.

Mendez, A., Islam, R., Latypov, T., Basa, P., Joseph, O., Knudsen, B., Siddiqui, A.M., Summer, P., Staehnke, L.J., Grahn, P.J., et al. (2020). Segment-specific orientation of the dorsal and ventral roots for precise therapeutic targeting of human spinal cord. Preprint at bioRxiv. https://doi.org/10.1101/2020.01.31.928804.

Milosevic, M., Masugi, Y., Sasaki, A., Sayenko, D.G., and Nakazawa, K. (2019). On the reflex mechanisms of cervical transcutaneous spinal cord stimulation in human subjects. J. Neurophysiol. *121*, 1672–1679.

Minassian, K., and Hofstoetter, U.S. (2016). Spinal cord stimulation and augmentative control strategies for leg movement after spinal paralysis in humans. CNS Neurosci. Ther. *22*, 262–270.

Moreno-Lopez, Y., Bichara, C., Delbecq, G., Isope, P., and Cordero-Erausquin, M. (2021). The corticospinal tract primarily modulates sensory inputs in the mouse lumbar cord. Elife *10*, e65304.

Omrani, M., Murnaghan, C.D., Pruszynski, J.A., and Scott, S.H. (2016). Distributed task-specific processing of somatosensory feedback for voluntary motor control. Elife *5*, e13141.

Pierrot-Deseilligny, E., and Burke, D. (2005). The Circuitry of the Human Spinal Cord: Its Role in Motor Control and Movement Disorders (Cambridge University Press).

Roberts, B.W.R., Atkinson, D.A., Manson, G.A., Markley, R., Kaldis, T., Britz, G.W., Horner, P.J., Vette, A.H., and Sayenko, D.G. (2021). Transcutaneous spinal cord stimulation improves postural stability in individuals with multiple sclerosis. Mult. Scler. Relat. Disord. *52*, 103009.

Rowald, A., Komi, S., Demesmaeker, R., Baaklini, E., Hernandez-Charpak, S.D., Paoles, E., Montanaro, H., Cassara, A., Becce, F., Lloyd, B., et al. (2022). Activity-dependent spinal cord neuromodulation rapidly restores trunk and leg motor functions after complete paralysis. Nat. Med. *28*, 260–271.

Roy, F.D., Gibson, G., and Stein, R.B. (2012). Effect of percutaneous stimulation at different spinal levels on the activation of sensory and motor roots. Exp. Brain Res. *223*, 281–289.

Sauerbrei, B.A., Guo, J.-Z., Cohen, J.D., Mischiati, M., Guo, W., Kabra, M., Verma, N., Mensh, B., Branson, K., and Hantman, A.W. (2020). Cortical pattern generation during dexterous movement is input-driven. Nature *577*, 386–391.

Sayenko, D.G., Angeli, C., Harkema, S.J., Edgerton, V.R., and Gerasimenko, Y.P. (2014). Neuromodulation of evoked muscle potentials induced by epidural spinal-cord stimulation in paralyzed individuals. J. Neurophysiol. *111*, 1088–1099.

Sayenko, D.G., Atkinson, D.A., Dy, C.J., Gurley, K.M., Smith, V.L., Angeli, C., Harkema, S.J., Edgerton, V.R., and Gerasimenko, Y.P. (2015). Spinal segment-specific transcutaneous stimulation differentially shapes activation pattern among motor pools in humans. J. Appl. Physiol. *118*, 1364–1374.

Sayenko, D.G., Rath, M., Ferguson, A.R., Burdick, J.W., Havton, L.A., Edgerton, V.R., and Gerasimenko, Y.P. (2019). Self-assisted standing enabled by non-invasive spinal stimulation after spinal cord injury. J. Neurotrauma *36*, 1435–1450.

Steele, A.G., Atkinson, D.A., Varghese, B., Oh, J., Markley, R.L., and Sayenko, D.G. (2021). Characterization of spinal sensorimotor network using transcutaneous spinal stimulation during voluntary movement preparation and performance. J. Clin. Med. *10*, 5958.

Taccola, G., Sayenko, D., Gad, P., Gerasimenko, Y., and Edgerton, V.R. (2018). And yet it moves: recovery of volitional control after spinal cord injury. Prog. Neurobiol. *160*, 64–81.

Taylor, C., McHugh, C., Mockler, D., Minogue, C., Reilly, R.B., and Fleming, N. (2021). Transcutaneous spinal cord stimulation and motor responses in individuals with spinal cord injury: a methodological review. PLoS One *16*, e0260166.

Taylor, J.L., and Gandevia, S.C. (2004). Noninvasive stimulation of the human corticospinal tract. J. Appl. Physiol. *96*, 1496–1503.

Wagner, F.B., Mignardot, J.B., Le Goff-Mignardot, C.G., Demesmaeker, R., Komi, S., Capogrosso, M., Rowald, A., Seáñez, I., Caban, M., Pirondini, E., et al. (2018). Targeted neurotechnology restores walking in humans with spinal cord injury. Nature *563*, 65–71.

STAR★METHODS

KEY RESOURCES TABLE

REAGENT or RESOURCE	SOURCE	IDENTIFIER
Software and algorithms		
MATLAB R2020a	Mathworks	https://www.mathworks.com
OriginPro 2021	Origin Lab	https://www.originlab.com

RESOURCE AVAILABILITY

Lead contact

Further information and requests should be directed to and will be fulfilled by the lead contact, Dimitry Sayenko (dgsayenko@houstonmethodist.org).

Materials availability

This study did not generate new materials or new unique reagents.

Data and code availability

- All data reported in this paper will be shared by the lead contact upon request.
- This paper does not report original code.
- Any additional information required to reanalyze the data reported in this paper is available from the lead contact upon request.

EXPERIMENTAL MODEL AND SUBJECT DETAILS

Human subjects

Eleven neurologically intact individuals (6 men and 5 women; age: 26.6 ± 4.9 years old, height: 176.6 ± 8.3 cm, weight: 75.3 ± 8.2 kg; see Table S1) were recruited to participate in this study. At the time of the study, they were free of any known history of neuromuscular disorder and/or musculoskeletal impairments. All study procedures were approved by the Houston Methodist Research Institute's Institutional Review Board, and all participants provided written informed consent.

METHOD DETAILS

Cervical transcutaneous spinal stimulation

During the experiments, the participants were in a seated position with their forearms supported anteriorly on a table. TSS was delivered using a constant current stimulator, DS8R (Digitimer Ltd, UK), with a sixteen-electrode array (ReCure™, Anuevo, CA, USA). The electrode array consisting of eight 10 mm and eight 20 mm diameter electrodes were used as cathodes (Figure 1B). The array was placed on the skin of each participant, over the cervical spinal cord and encompassed the area between the C4 and T1 spinous processes. The electrode EL15 was placed midline at C7-T1 spinous processes. Two 5×9 cm self-adhesive rectangular anodes (Axelgaard Manufacturing Co. Ltd., USA) were placed on the anterior iliac crests of each participant.

Double-pulse TSS was delivered using a pair of monophasic pulses of 500 μs duration, with inter-stimuli interval of 30 ms. The use of double-pulse TSS provides confirmation of the reflex nature of the spinally evoked motor responses by exhibiting a reduction of the second evoked potential amplitude in a previously activated sensory-motor synapse, which is attributed to post-activation- or homosynaptic-depression (Andrews et al., 2015; Hofstoetter et al., 2020; Roy et al., 2012; Steele et al., 2021). This can distinguish responses evoked transsynaptically through the dorsal roots (i.e., via the sensory route) from the responses evoked due to activation of motor axons within the ventral roots, which are not susceptible to any conditioning influences including afferent or descending inputs (Taylor and Gandevia, 2004). Stimulation began at 20 mA and was increased by increments of 5 mA to 150 mA or to the maximum tolerated intensity (see Tables S2 and S3). One stimulus was delivered for each intensity to minimize stimulation discomfort.

Stimulation was applied at each of the rostrocaudal (EL03, EL07, EL11, EL15), rostral mediolateral (EL01, EL02, EL03, EL04, EL05) and caudal mediolateral (EL09, EL10, EL11, EL12, EL13) sites (Figure 1B).

EMG recording and data collection

Trigno Avanti wireless surface electromyography (EMG) electrodes (Delsys Inc., USA; common-mode rejection ratio <80 dB; size: 27 mm x 37 mm x 13 mm; input impedance: > 1015 Ω/0.2 pF) were placed bilaterally and symmetrically at six sites: biceps brachii (BIC), triceps brachii (TRI), flexor carpi radialis (FCR), extensor carpi radialis (ECR), abductor pollicis brevis (APB), and abductor digiti minimi (ADM) muscles. EMG data was amplified using a Trigno Avanti amplifier (Delsys Inc.; gain: 909; bandwidth: 20 to 450 Hz) and recorded at a sampling frequency of 2,000 Hz using a PowerLab data acquisition system (ADInstruments, Australia).

Data processing and analysis

Motor threshold

Data were processed using LabChart Pro 8.1.13 software (ADInstruments, Australia). For each muscle, the response was calculated by measuring the peak-to-peak amplitude within a 20-ms window 5 ms from stimulus onset. Motor threshold (MT) was defined as the first amplitude that created a response greater than 20 μV (Calvert et al., 2019). The evoked response was normalized to the MT of FCR during stimulation at the EL07 (FCR at EL07 = 1.0). To visualize the selectivity of the activation of motor pools projecting to proximal and distal UL muscles, a heatmap was constructed by bilinear interpolation. A total 55 of color levels were used with 5 major and 10 minor levels using the normalized MT stimulation intensity values during stimulation along the rostrocaudal axis. Based on known anatomical maps and interjacent location of the FCR motor pools in the cervical enlargement (Figure 1A), we suggested that FCR motor pools would be always activated, irrespective of either rostral or caudal placement of the stimulating electrode. As such, we normalized the response in studied UL muscles by the FCR response.

Recruitment curves

Recruitment curves were generated using the peak-to-peak EMG amplitude at each stimulation intensities for all tested muscles. The recruitment curves were obtained by increasing stimulation intensity by 5 mA starting at 20 mA until maximum tolerated intensity. Post processing was performed using a custom code written in MATLAB R2020a (MathWorks, Natick, MA). Recruitment curves for each muscle were normalized to the MaxR across all stimulation sites.

Post-activation depression (R2/R1 ratio)

The ratio between the second (R2) and the first (R1) responses was calculated (Milosevic et al., 2019). The R2/R1 ratio below 1 indicates that the second response was suppressed by the first stimulus, and therefore affirms the presence of post-activation depression. The minimum R2/R1 values, that is when the largest difference between the R2 and R1 responses occurred, were chosen for comparison across different stimulation sites for each muscle individually.

Motor activation patterns of rostrocaudal and mediolateral stimulation sites

Parallel coordinate plots were constructed using the MaxR of each analyzed muscle in different stimulation sites to visualize the relative selectivity of the recruitment of different motor pools along the rostrocaudal axis of the cervical enlargement. Each individual stimulation site was assigned its own axis with an independent scale based on the MaxR values.

We also constructed heatmaps demonstrating motor recruitment from 20 mA to 100 mA or the maximum tolerated intensity to investigate preferential activation of mediolateral stimulation sites on motor recruitment for left and right BIC, FCR, and APB muscles. Individual data were normalized to the participants' maximum evoked potential then pooled for analysis.

Probability of motor activation

To determine the comprehensive information of probability of motor activation from a specific stimulation site, and to infer the segmental distributions of the dorsal roots and motor pools projecting to the recorded UL muscles, the mean rank value was calculated based on MT, MaxR, and R2/R1 ratio. From practical standpoint, the probability maps reflect the interplay between the MT, MaxR, and R2/R1 ratio because the ensemble of these variables, rather than each separate parameter, highlights the characteristics of evoked

responses at different stimulation locations and guides spinal mapping. In addition, there was weak correlation between MT and MaxR at given stimulation sites based on Pearson's correlation analysis ($r = 0.136$, $p = 0.027$). Thus, taking each variable into account gives a more inclusive understanding of the characteristics of evoked responses and activation of given muscles. The mean rank value of these three variables was determined using a Kruskal-Wallis test for each variable. Each of the mean rank values of MT, MaxR, and R2/R1 ratio were summed together to acquire the total score values. The total score of these three variables were then normalized from the maximum score for each muscle to determine the probability of muscle activation patterns along the rostrocaudal, rostral mediolateral, and caudal mediolateral axes.

QUANTIFICATION AND STATISTICAL ANALYSIS

All statistical analyses were performed using OriginPro 2021 (Origin Lab Corporation, Northampton, MA, USA). Assumptions of normality were tested using the Shapiro-Wilk test. Normally distributed data were analyzed using the two-way analysis of variance (ANOVA) to evaluate MT, MaxR, and R2/R1 ratio differences between all tested UL muscles and stimulation sites. Data were corrected for multiple comparisons within figures using a Holm-Bonferroni's *post hoc* test. Non-normally distributed data were analyzed with a Kruskal–Wallis test followed by Dunn's multiple comparison test. p values <0.05 were considered significant (*$p < 0.05$, **$p < 0.01$ and ***$p < 0.001$). One participant was unable to complete the experiment due to discomfort; therefore, the corresponding sample of muscle responses (at EL02, EL04, EL10, & EL12) for that participant was not included during statistical analysis.

We compared the responses in left limb muscles during rostrocaudal stimulation sites. For mediolateral stimulation sites, we analyzed responses from the left limb only when stimulation was performed using left-sided electrodes (EL01, EL02, EL09, EL10), and the right limb only during stimulation using right-sided electrodes (EL04, EL05, EL12, EL13). The MaxR was calculated as the average of the three largest evoked response values in Figures 3E and 7C and 7D. In order to determine preferential activation of rostrocaudal stimulation sites on motor recruitment, the MaxR was normalized using the maximum peak-to-peak amplitude across muscles for that stimulation site to determine selectivity in activation. For the mediolateral axes, the MaxR were normalized to the midline electrodes: EL03 for rostral mediolateral and EL11 for caudal mediolateral comparisons. The MT was normalized at the same location FCR, EL07 for the mediolateral comparison.